JOURNAL OF QUATERNARY SCIENCE (2009) **24**(1) 33–45

Published online 6 March 2008 in Wiley InterScience
(www.interscience.wiley.com) DOI: 10.1002/jqs.1166

Holocene climate inferred from glacier extent, lake sediment and tree rings at Goat Lake, Kenai Mountains, Alaska, USA

THOMAS A. DAIGLE and DARRELL S. KAUFMAN*
Northern Arizona University, Department of Geology, Flagstaff, Arizona, USA

Daigle, T. A. and Kaufman, D. S. 2009. Holocene climate inferred from glacier extent, lake sediment and tree rings at Goat Lake, Kenai Mountains, Alaska, USA. *J. Quaternary Sci.*, **Vol. 24** pp. 33–45. ISSN 0267-8179.

Received 24 May 2007; Revised 24 November 2007; Accepted 6 December 2007

ABSTRACT: Lake sediment, glacier extent and tree rings were used to reconstruct Holocene climate changes from Goat Lake at 550 m asl in the Kenai Mountains, south-central Alaska. Radiocarbon-dated sediment cores taken at 55 m water depth show glacial-lacustrine conditions until about 9500 cal. yr BP, followed by organic-rich sedimentation with an overall increasing trend in organic matter and biogenic silica content leading up to the Little Ice Age (LIA). Through most of the Holocene, the northern outlet of the Harding Icefield remained below the drainage divide that currently separates it from Goat Lake. A sharp transition from gyttja to inorganic mud about AD 1660 signifies the reappearance of glacier meltwater into Goat Lake during the LIA, marking the maximum Holocene (postglacial) extent. Meltwater continued to discharge into the lake until about AD 1900. A 207 yr tree-ring series from 25 mountain hemlocks growing in the Goat Lake watershed correlates with other regional tree-ring series that indicate an average summer temperature reduction of about 1°C during the 19th century compared with the early–mid 20th century. Cirque glaciers around Goat Lake reached their maximum LIA extent in the late 19th century. Assuming that glacier equilibrium-line altitudes (ELA) are controlled solely by summer temperature, then the cooling of 1°C combined with the local environmental lapse rate would indicate an ELA lowering of 170 m. In contrast, reconstructed ELAs of 12 cirque glaciers near Goat Lake average only 34 ± 18 m lower during the LIA. The restricted ELA lowering can be explained by a reduction in accumulation-season precipitation caused by a weakening of the Aleutian low-pressure system during the late LIA. Copyright © 2008 John Wiley & Sons, Ltd.

KEYWORDS: tree rings; equilibrium-line altitude; lake sediment; Little Ice Age; Holocene climate change; Alaska.

Introduction

Broad-scale climate forcing leads to climatic changes on a variety of spatial and temporal scales. Understanding decadal- to millennial-scale climate variability at a regional scale requires a dense network of proxy climate indicators. Because each proxy reflects different environmental variables and temporal responses, multiple proxies are needed to develop a more complete understanding of past climate variability. Changes in lake sediment, glacier size, and tree-ring widths afford complementary evidence for past temperature and precipitation fluctuations during the Little Ice Age (LIA) (Osborn *et al.*, 2007). Here we present a multi-proxy analysis of Holocene climate records from the Goat Lake area in the Kenai Mountains of south-central Alaska. Goat Lake lies at the northern margin of the Harding Icefield, where it is uniquely situated to record the thickness of an outlet glacier through an on/off glacial meltwater signal (Fig. 1). The lake is currently separated from the outlet glacier by a low drainage divide, but during times when the glacier thickened to the threshold of the basin, it discharged meltwater directly into Goat Lake.

In this study we: (1) evaluate sediment cores from Goat Lake with respect to climate and glaciation; (2) reconstruct the maximum extent of cirque glaciers during the LIA to estimate the associated amount of equilibrium-line altitude (ELA) lowering; (3) compare a new tree-ring series from the Goat Lake drainage basin with other nearby dendroclimatological studies; and (4) combine our records to understand precipitation change related to north Pacific atmospheric circulation during the LIA maximum. This research builds on the extensive prior studies of late Holocene climate change around the Gulf of Alaska based on glacier fluctuations and tree-ring chronologies (e.g. Wiles *et al.*, 2008). Our multi-proxy study places climate variability of the LIA into a longer-term perspective of Holocene change. The results of our research illuminate the influence of atmospheric circulation changes on temperature and precipitation change around the Kenai Peninsula. In

* Correspondence to: D. S. Kaufman, Department of Geology, Northern Arizona University, Flagstaff, AZ 86011-4099, USA.
E-mail: darrell.kaufman@nau.edu

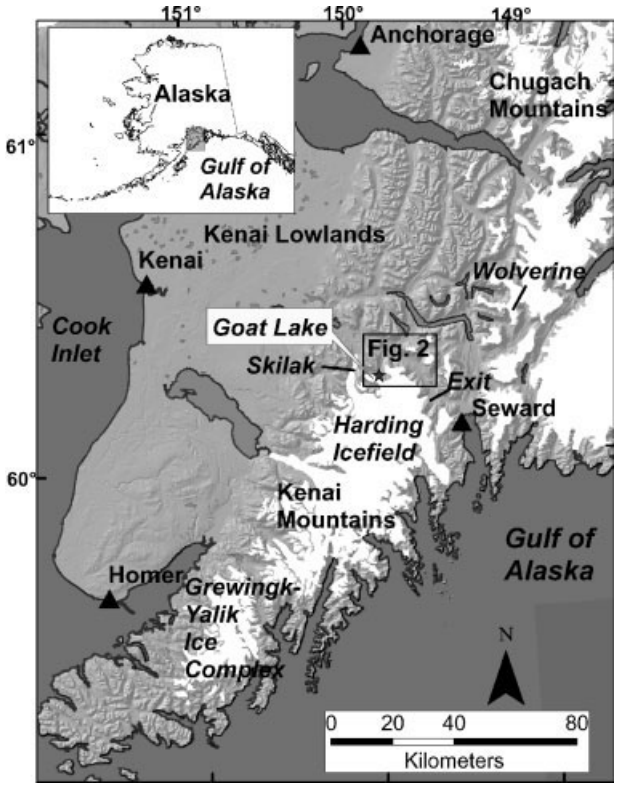

Figure 1 Kenai Peninsula showing Goat Lake and other locations discussed in the text

addition, we contribute to a growing database of palaeoclimate data from southern Alaska and elsewhere around the north-eastern Pacific that provides a framework for understanding late Holocene climate changes, including 20th century warming.

Study area

The Kenai Mountains form the backbone of the Kenai Peninsula, separating the Gulf of Alaska to the south from Cook Inlet to the west (Fig. 1). The range reaches elevations of 2000 m above sea level (asl) and supports numerous ice fields and mountain glaciers. The Harding Icefield is the largest, covering ~1800 km^2, with 31 land-terminating outlet glaciers and seven tidewater glaciers. The range forms an effective precipitation barrier, with the western Kenai Peninsula receiving significantly less precipitation (490 mm yr^{-1} at Kenai) than the east (1660 mm yr^{-1} at Seward); mean annual temperature is also lower in the west (1.1°C at Kenai; 4.1°C at Seward) (Western Regional Climate Center, 2006).

The climate of the Kenai Peninsula is strongly influenced by the Aleutian low-pressure system, especially in the winter when it controls cyclonic circulation over the north-east Pacific Ocean and steers storms into the Gulf of Alaska (Rodionov *et al.*, 2005). In addition to seasonal migration, the Aleutian low has two primary decadal modes: positive when the system is generally more easterly and intense (i.e. lower central sea-level pressures), and negative when the system is generally more westerly weak (Overland *et al.*, 1999). The intensity of the Aleutian low is related to larger-scale atmospheric circulation phenomena such as the Pacific Decadal Oscillation, the Pacific North American Pattern and the Arctic Oscillation (Overland *et al.*, 1999; Minobe and Mantua, 1999; D'Arrigo *et al.*, 1999; Papineau, 2001). Prolonged positive Aleutian low phases have been correlated with warmer temperature and increased winter precipitation along the Gulf of Alaska and northwestern North America (Anderson *et al.*, 2005).

Goat Lake (60.2583° N, 149.9083° W) is located at 550 m asl in the central Kenai Mountains, about 1 km north of an outlet of the northern Harding Icefield, and 45 km northwest of Seward (Fig. 1). The lake (0.38 km^2) is 55 m deep and occupies a small catchment (2.8 km^2) in an overdeepened, glacially scoured basin (Fig. 2). It is contained by a bedrock sill at the northern outlet, and drains into Upper Russian Lake. The lake currently receives limited perennial surface-water inflow; the main input emanates from a small pond 200 m east of the lake. Mountain summits rise to 1460 m within 5 km of the lake. Vegetation in the Goat Lake drainage basin is dominated by alder (*Alnus incana sinuata*) with mountain hemlock (*Tsuga mertensiana*), Sitka spruce (*Picea sitchensis*), shrub birch (*Betula nana*), ferns and grasses.

Glacial-geological mapping and lichenometry

Twelve cirque glaciers within 23 km of Goat Lake (Fig. 2) were selected for glacial-geological mapping based on their relatively small size (3.5–0.2 km^2; average = 0.9 km^2; Table 1), well-defined margins and topographic confinement, which simplifies assumptions related to ELA reconstructions and glacier response times. Glacial geomorphic features that delimit former ice margins were mapped on 1:63 000-scale US Geological Survey maps and digitised in ArcMap (v9). Because ice-marginal features are generally sparse in the accumulation areas, we projected lateral moraines or trimlines up-valley to where they intersected the glacier boundaries shown on the US Geological Survey maps. Photography for these maps was flown in August 1950.

Field mapping and lichen measurements were made in July 2005 in the forefields of two cirque glaciers (cirques 2 and 12; Fig. 2) and at the drainage divide. Other glaciers were inaccessible by foot and we relied on aerial photo-interpretative mapping. A lichen growth curve previously developed for the genus *Rhizocarpon* in the Kenai Mountains (Solomina and Calkin, 2003) was used to determine the approximate age of ice-marginal surfaces near Goat Lake, namely:

$$t = 20.245 + 2.1035D$$

where D = thallus diameter (mm), and t = age of the lichen (years before 1950 = BP). Following the methods used to derive the growth curve, we used the long axis of the single largest, approximately circular *Rhizocarpon* lichen from each surface to calculate the age (Solomina and Calkin, 2003). The accuracy of lichenometric ages is about 15–20% (Calkin and Ellis, 1980).

Cirque 2 contains a 0.6 km long glacier that descends to 1000 m asl. Its forefield is marked by a well-defined outer moraine with multiple discontinuous inner-moraine ridges. Large, flat rock surfaces with lichen are suitable for lichenometry and were found near the upper limit of the left lateral moraine, on the terminal moraine, and on the right lateral moraine. The lichen sizes at all three locations are similar, and suggest an age of about AD 1890 ± 15 for the stabilisation of the outermost moraine. Like other glaciers in the study area, the glacier terminus at cirque 2 retreated 200 m since 1950 (4 m yr^{-1}), compared to about 500 m from the LIA to AD 1950.

Cirque 12 is the lowest, easternmost maritime-influenced glacier mapped in this study. The cirque supports a 0.7 km long glacier that descends to 800 m asl. The outermost moraine is

DOI: 10.1002/jqs

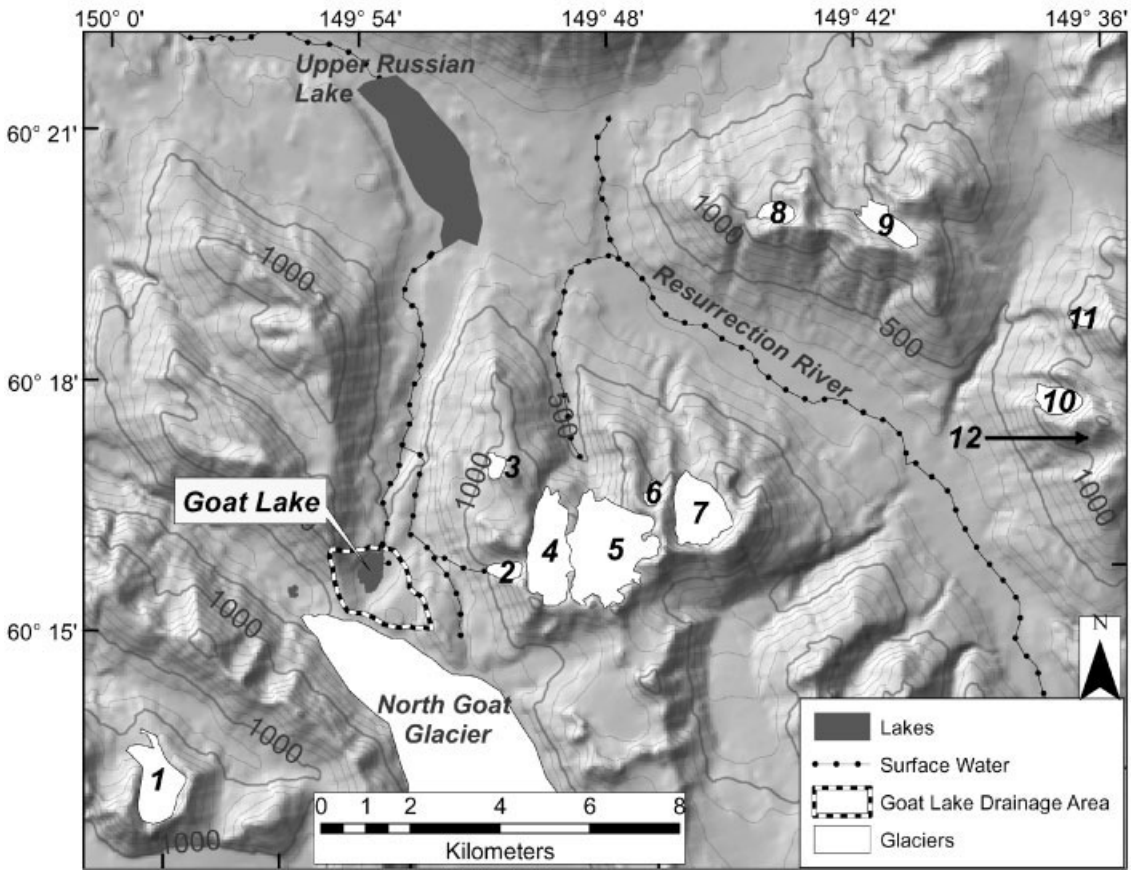

Figure 2 Goat Lake study area showing the glaciers (1–11 from west to east) used to estimate equilibrium-line altitudes. Their extent is based on 1950 aerial photography as shown on US Geological Survey maps. Cirque 12 is located 23 km east of Goat Lake

about 40 m tall, with a continuous sharp-crested ridge that extends well into the main valley and encompasses several smaller, ice-cored moraines. The outer moraine is over-steepened and two suitable surfaces for lichenometry were found just inside the left and right lateral moraine crests on smaller, inset moraines. Lichen sizes at these stations suggest an age of about AD 1930 for the stabilisation of the inset moraines, which were deposited following the LIA. The approximate age of the outermost moraine is AD 1820 on the basis of a single lichen station just inside the outer crest where the moraine bulges to the north-west.

The results from these two cirque glaciers confirm that the outermost unvegetated moraines in these valleys were formed during the latter part of the LIA. This is consistent with previous work in the area by Wiles and Calkin (1993, 1994), Padginton (1993) and Calkin *et al.* (2001), who demonstrated that most glaciers in the Kenai Mountains reached their Holocene maximum positions late during the 19th century. Similar ice-marginal features of 10 other nearby, inaccessible cirques were identified using false-colour infrared aerial photos (flown in August 1986; 1:63 000 scale) and are assumed to have formed late during the LIA.

In addition to the local cirque glaciers, we mapped ice-marginal features and measured lichen sizes along the right-lateral margin of an outlet glacier emanating from the Harding Icefield, which we refer to here as the North Goat Glacier (NGG) to distinguish it from the Goat Glacier, which discharges from the south-west end of the icefield. The NGG is located between the Skilak and Exit glaciers. The glacier extends 17 km from the ice divide and terminates on bare bedrock draped with thin drift and detrital logs. The valley walls are marked by a distinct trimline that merges down-valley with a small, discontinuous end moraine (Fig. 3). The NGG is currently separated from Goat Lake by a drainage divide located 450 m south and 70 m above the lake. The glacier surface is currently 150 m below the drainage divide.

Glacial-geological mapping at the divide provides some constraints on the ice configuration during the LIA. A low-relief (1–2 m), sinuous ridge blanketed by 0.5–1.0 m of silt densely rooted by grass forms the outermost moraine. The moraine is cored by angular clasts up to 1 m in diameter in a sandy matrix. It is located a few metres outside the modern vegetation trimline and remains undated because it lacks surface boulders for lichenometry, and a test pit did not reveal any obvious tephra layers. The lowest point of the drainage divide located just south of the outermost moraine is marked by two bouldery outwash bars with imbricated clasts that indicate flow towards Goat Lake. Each deposit is 1–2 m high, 20 m across and 30 m long. They form the head of an outwash channel that fed Goat Lake when the ice margin occupied the divide. Lichens on both surfaces are of similar size, with a maximum diameter of 37 mm, corresponding to an age of AD 1910 (Fig. 3).

Several discontinuous, low-relief (0.5–1 m high), rocky moraines mark the terrain just inside the trimline and outwash bars. Lichens on the outer moraine reach 46 mm, corresponding to an age of AD 1890 (Fig. 3). Inset moraines were deposited following the retreat of ice below the drainage divide. Lichen measurements on bedrock in the NGG valley near the LIA terminal margin indicate an age of AD 1920. We settle on an age of AD 1900 for the retreat of the NGG below the drainage divide.

Equilibrium-line altitudes

Equilibrium-line altitudes (ELA) for cirque glaciers near Goat Lake were calculated using the accumulation–area ratio (AAR)

DOI: 10.1002/jqs

Table 1 Central Kenai Mountains cirque glacier equilibrium-line altitudes

Glacier (Fig. 2)	Aspect	Location		1950 (AD)				Little Ice Age (ca. 1800–1900 AD)					Area lost (%)
		Lat. (60° N)	Lon. (149 °W)	Length[a] (km)	Area[a] (km^2)	ELA[b] (m)	Error[c]	Length[a] (km)	Area[a] (km^2)	ELA[b] (m)	Error[c]	ΔELA (m)	
1	N	13′ 00″	59′ 56″	1.7	1.44	1185	10	2.8	2.06	1125	27	60	30
2	W	15′ 24″	51′ 10″	0.8	0.25	1115	13	1.1	0.37	1090	12	25	32
3	N	16′ 36″	51′ 17″	0.6	0.20	1085	9	1.0	0.37	1045	8	40	46
4	N	15′ 33″	48′ 38″	2.6	1.98	1090	16	3.1	2.37	1080	10	10	16
5	N	15′ 33″	50′ 15″	2.5	3.50	1115	15	3.2	3.90	1090	18	25	10
6	N	16′ 13″	47′ 35″	0.6	0.15	990	9	1.2	0.34	980	8	10	56
7	N	15′ 50″	46′ 30″	1.6	1.56	995	9	2.5	1.81	970	20	25	14
8	W	19′ 28″	43′ 59″	0.8	0.28	1020	9	1.3	0.57	970	9	50	51
9	W	19′ 13″	41′ 21″	1.4	0.69	1060	10	1.9	0.99	1025	14	35	30
10	W	17′ 00″	37′ 27″	1.0	0.51	953	8	1.4	0.67	940	11	13	24
11	W	17′ 58″	36′ 48″	0.6	0.17	1080	7	1.0	0.32	1025	14	55	47
12	N	15′ 57″	28′ 59″	0.9	0.30	840	12	1.4	0.49	785	14	55	39
Average	NW			1.3	0.92	1044	11	1.8	1.19	1010	14	34	23
Standard deviation				0.7	0.98	87	3	0.8	1.08	88	5	18	15

[a] Length and area are from the mapped USGS (1951) extent (1950 photography).
[b] ELAs are based on AAR of 0.62.
[c] Error is determined by using a range of AAR from 0.55 to 0.65.

method (e.g. Benn *et al.*, 2005). The method assumes steady-state glacier mass balance and is based on former glacier extent mapped from ice-marginal geomorphic features. In this study, palaeo-glacier surface contours were drawn using ArcMap (v9), consistent with the principles of glacier flow (concave up-glacier in the ablation area and convex in the accumulation area), and the area between contour intervals was summed to generate an area–altitude plot from which the ELA was estimated. We compare palaeo-glacier morphology with modern glacier contours depicted on 1950 USGS topographic maps.

We assume a modern (1950) AAR of 0.62 for the 12 cirque glaciers in our study area based on mass-balance measurements from 1966 to 2002 at Wolverine Glacier located 50 km north-east of Goat Lake (http://ak.water.usgs.gov/glaciology/all_bmg/3glacier_balance.htm [accessed 24 September 2007]). Of the three glaciers in Alaska with the longest-term mass-balance records, Wolverine Glacier is the closest, although it is expected to have higher annual precipitation than the glaciers around Goat Lake owing to its location on the coastal side of the Kenai Mountains (Fig. 1). Applying an AAR of 0.62 indicates that the AD 1950 ELA was 1044 ± 87 m (Table 1). The error is calculated as the standard deviation of the 12 individual values. It is eight times larger than the average uncertainty estimated for individual glaciers by applying a range of reasonable AAR values (Table 1) and probably reflects the influence of snow drift, shading and other important microclimate effects on the ELA. Applying the same AAR to reconstructed LIA glaciers results in an ELA of 1010 ± 88 m, or 34 ± 18 m lower than modern (= ΔELA).

Because our ΔELA estimate depends to some extent on the choice of AAR, we evaluated the ELA for a range of AAR values. Moraines deposited during the LIA imply glacier equilibrium with contemporaneous climate, whereas in 1950 the glaciers were not depositing moraines and were probably retreating in response to general post-LIA warming of the first half of the 20th century. Therefore the AAR of the reconstructed LIA glaciers may have been higher than for the 1950 glaciers, whose geometry reflects an integrated average of the mass balance during the few decades (estimated response time) prior to 1950.

AARs for alpine glaciers in a global dataset (Duyergerov, 2002) typically range from 0.55 to 0.65. To estimate the maximum ΔELA value, we assume that AAR was higher (0.65) for the LIA glaciers and lower (0.55) for the 1950 glaciers, resulting in a ΔELA estimate of 60 ± 20 m. This is a maximum value because the AAR during the decades before 1950 was probably not significantly lower than the 1966–2002 average of 0.62 for Wolverine Glacier. We infer that the AAR of glaciers photographed in 1950 was close to 0.62 based on the strong correlation ($r = 0.64$; $P = 4.77 \times 10^{-5}$) between total winter precipitation (October through March) at Seward airport (period of record = 1922–2005) and the AAR measured at Wolverine Glacier from 1966–2002, which we use to estimate the ELA for the decades prior to 1950. Because the AAR of the LIA and the 1950 glaciers was similar, the ΔELA is probably closer to 34 m than to 60 m. Furthermore, the elevations inferred for the reconstructed LIA glaciers were based on the 1950 glacier topography. Because the surface of the glaciers was somewhat higher during the LIA, our ELA estimates for the LIA underestimate the true ELA, and therefore the ΔELA values are probably too large. For example, increasing the accumulation area by 10% and the elevation by 20 m increased the reconstructed ELA by about 6 m for a typical cirque glacier around Goat Lake (Daigle, 2006).

A 34–60 m ΔELA for the LIA is lower than previous estimates from the Kenai Mountains. Wiles (1992) reported a ΔELA of 100–150 m compared to the late 20th century (1980s), and Padginton (1993) estimated a ΔELA of 90 m relative to 1950. Wiles' value was based on a different procedure and cannot be compared directly to our estimates. Padginton's ELA reconstruction, however, was obtained using the AAR method, similar to this study. He studied the Grenwingk-Yalik Ice Complex, about 90 km southwest from Goat Lake, where climate change is unlikely to have been significantly different. We suggest the different ΔELA estimates reflect uncertainties associated with applying the AAR technique to large, complex ice masses with shifting ice divides, which introduces some error that is otherwise partially controlled when using smaller, topographically confined glaciers as in this study. Although Wiles (1992) and Padginton (1993) report a ΔELA that is two to five times higher than our estimate from the same mountain range, our results are consistent with other recent studies of ΔELA in southern Alaska during the LIA. For example, Levy *et al.* (2004) estimated a ΔELA of 35 ± 22 m for the Ahklun

DOI: 10.1002/jqs

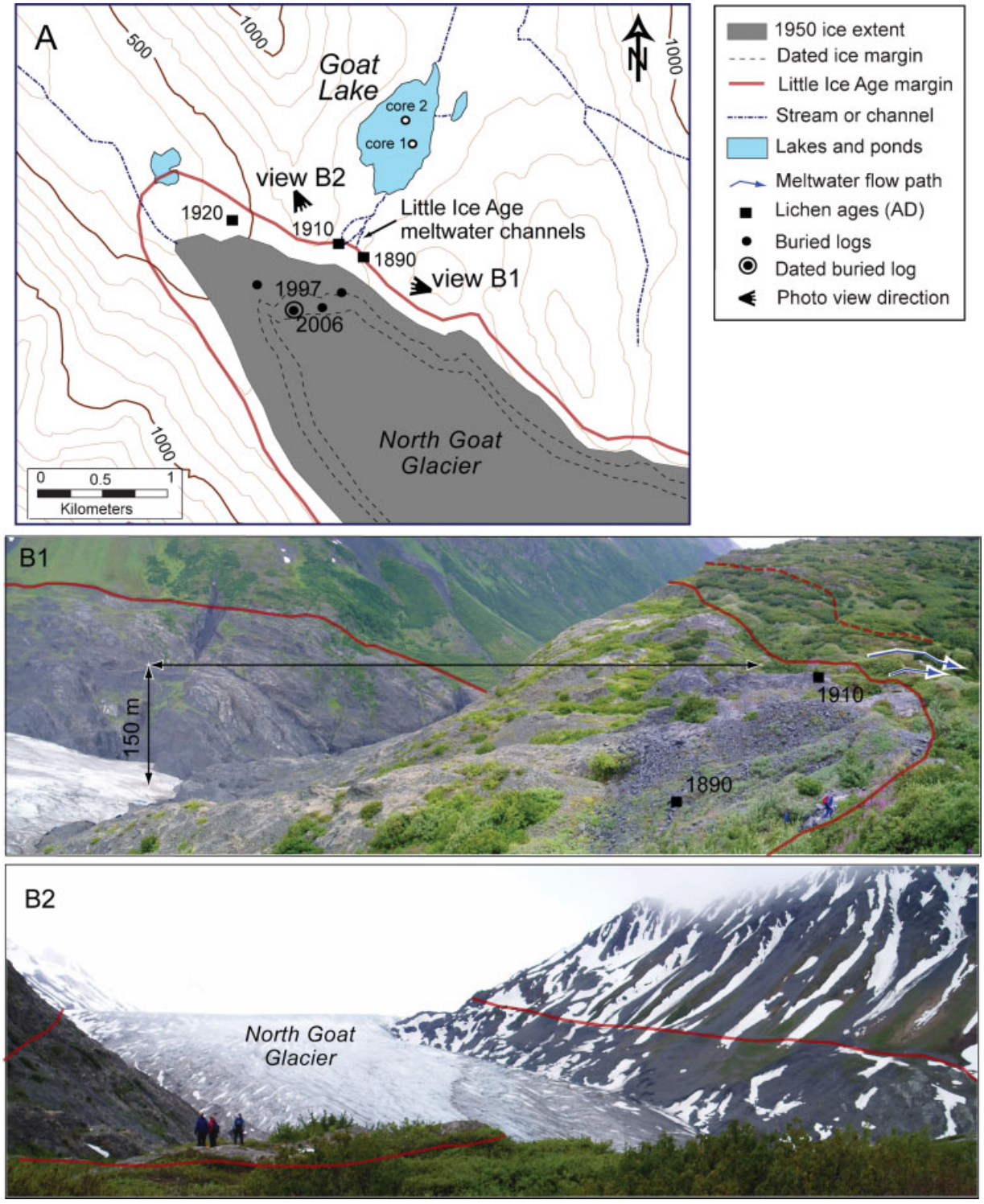

Figure 3 (A) Valley of the North Goat Glacier showing glacier extent during 1950, 1997, and 2006, Little Ice Age (LIA) margin, outwash channels, lichen sites and locations of subfossil trees. (B) View of drainage divide looking down-valley (view B1) and up-valley (view B2) showing the LIA margins and lichen stations with ages. Dashed line is the maximum LIA extent marked by the outer grass-covered moraine. The solid line indicates the margin associated with meltwater outwash bars and an unvegetated moraine with a lichenometric age of about 1900 AD

Mountains of south-west Alaska, similar to Kathan's (2006) value of 23 ± 13 m from Ahklun Mountains, but somewhat lower than McKay's (2007) estimate of 83 ± 46 m from the central Chugach Range.

Lake sediment

Goat Lake fills a simple, flat-bottomed basin reaching a maximum depth of 55 m (Fig. 4). Sub-bottom acoustic images indicate a consistent, sub-parallel sedimentary sequence through the deepest part of the basin with a maximum thickness of 4 m. Core site 1 is located near the deepest part of the lake, where sedimentation rates are presumably the highest. Core site 2 is located 200 m north of core 1. Sediment analyses were done primarily on core 1 owing to its somewhat better preservation.

Lake sediment properties, including organic matter content (OM), biogenic silica (BSi) and magnetic susceptibility (MS), reflect past limnological conditions and have been widely used as climate proxies in high-latitude lakes because they respond

DOI: 10.1002/jqs

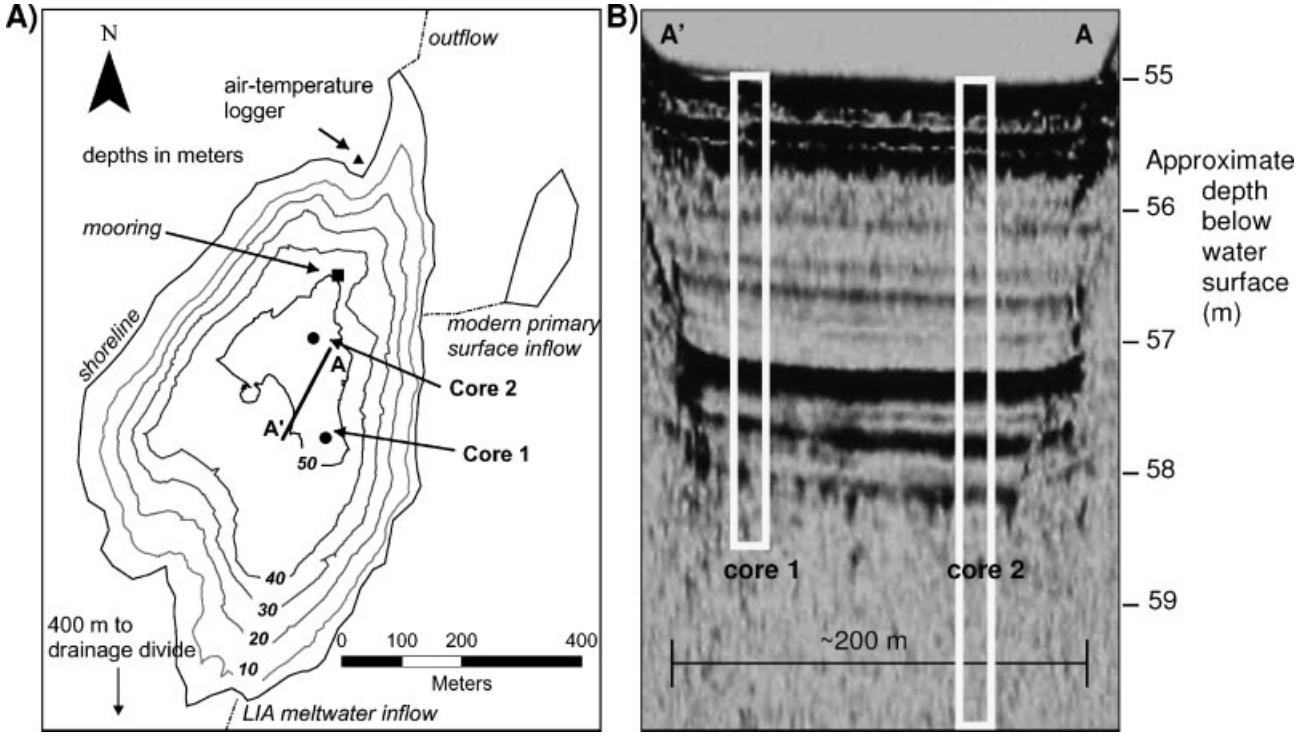

Figure 4 (A) Goat Lake bathymetric map showing location of core sites, air-temperature logger and acoustic stratigraphic transect. (B) Acoustic sub-bottom profile. Depths are approximate due to uncertainties in acoustic travel time and the strength of various sedimentary reflectors. Dark reflectors from 55.5 to 55.0 m represent transitions from organic-rich to inorganic mud. Dark reflectors from 58.0 to 55.5 m represent tephra beds. The lack of reflectors below 58 m indicates massive, inorganic mud

quickly and sensitively to environmental changes (e.g. Hu *et al.*, 2003; Nesje *et al.*, 2004). OM was measured on core 1 at 1 cm intervals by weight loss on ignition after combustion at 550°C for 5 h. BSi was measured on core 1 every 1–4 cm depending on the stratigraphy. BSi content was determined on 50 mg of dried, crushed sediment by extraction with 10% Na_2CO_3 following the procedures of Mortlock and Froelich (1989). MS was measured every 0.5 cm on both cores 1 and 2 using a Bartington MS2E surface meter. The upper 3 cm from surface core 05-GT-2C (Fig. 4; core site 2) was sampled at 0.5 cm intervals for MS and OM, and 0.25 cm intervals for BSi. The interval from 3 to 8 cm of core 05-GT-2C was sampled at 0.5 cm intervals for MS, OM and BSi. All data from these analyses are in Daigle (2006).

Chronology

Sixteen accelerator mass spectrometry (AMS) ^{14}C ages were obtained from core 1 by removing 1 cm thick swaths of bulk sediment from selected depths and sieving through a 60 μm mesh. Vegetation macrofossils and, in some cases, insect chitin, were isolated under a binocular microscope. The samples were analysed by AMS at the Lawrence Livermore National Laboratory, and ^{14}C ages were calibrated using CALIB 5.0 (Stuiver and Reimer, 1993). All ages are reported as the median probability of the calibrated age range in calendar years BP (hereafter cal. yr BP). Errors are reported as ± one half of the 1σ calibrated age range (Table 2).

Several stratigraphic transitions in core 1 prohibit the application of a single, smooth age–depth relation. To derive an age model, we divided the core into two sections (298–56 cm and 56–0 cm; Fig. 5). The lower section of core 1 includes 10 ^{14}C ages that were fit with a second-order polynomial equation ($R^2 = 0.992$), indicating a decreasing sedimentation rate downward, consistent with sediment compaction. Five ^{14}C ages were rejected because they were significantly older than expected based on neighbouring ages, and are suspected to contain some portion of terrestrial bryophyte material. Both wood and terrestrial bryophytes (Daigle, 2006) from 34 cm depth were analysed separately, and the bryophytes dated 2000 yr older (Table 2). Terrestrial bryophytes could not be positively identified in the other four rejected samples, but we suspect that the old ages reflect the input of old vegetative material that washed into the lake centuries or millennia after death. Tephra accounts for 2% of the total sediment thickness, and does not significantly impact the age model of the lower part. The upper section was fit with four linear segments because different lithologies indicate markedly different sedimentation rates: (1) The tephra from 56–46 cm depth was presumed to have been deposited instantaneously around 715 cal. yr BP (AD 1235) based on the polynomial age model and the depth of the lower contact; (2) the interval of organic-rich gyttja above the tephra (46–34 cm) was fit with a linear age model from 715 to 290 cal. yr BP (AD 1660) based on a ^{14}C age on wood fragments at 34 cm; (3) the laminated inorganic interval from 34–3 cm was fit with a linear age model from AD 1660 to 1900, where the upper age was determined from the lichenometric age of the abandoned outwash channel at the drainage divide; (4) the gyttja from 3–0 cm was fit with a linear age model from AD 1900 AD to the present.

Lithostratigraphy

The sediment–water interface is rarely recovered in percussion coring, and short surface cores were used to splice together a longer record that included the upper sediment layers. Identical

DOI: 10.1002/jqs

Table 2 AMS ^{14}C ages from Goat Lake

Laboratory ID (CAMS #)[a]	Sample name	Depth (cm blf)[b]	^{14}C age (yr BP)	±	Calibrated median probability (yr BP)[c]	± 1/2 of 1σ range	Material[d]
114459	Core 1 26A[e]	34	1995	35	1945	70	Bryophytes
114460	Core 1 26B	34	245	35	292	130	Non-charred wood fragments
117534	Core 1 29.5[e]	37.5	2980	35	3168	70	Plant stems and some leaf fragments
117535	Core 1 35[e]	42–43	1300	45	1234	70	Unspecified plant fragments
114461	Core 1 51[e]	58–59	1250	35	1200	60	Small wood fragments and plant stems
114462	Core 1 73	81	1290	35	1230	50	Leaf
117536	Core 1 83	91–92	1500	35	1380	30	Unspecified plant fragments
114463	Core 1 100	108–109	2260	35	2240	80	Small leaf fragments, insect chiton, beetle elytra
114464	Core 1 136	142–143	3090	35	3315	50	Leaf fragments, unidentified plant stems
117537	Core 1 163[e]	171–172	4220	35	4750	90	Small wood chunks, unidentified plant fragments and minor chiton
114465	Core 1 183.5	191.5	4020	35	4485	45	Unspecified wood chunks
114466	Core 1 217.3	225–225.5	5085	35	5815	75	Unspecified plant fragments and insect chiton
114467	Core 1 223	231–232	5380	30	6205	75	Unspecified herbaceous plant material
120879	Core 1 232.5	240–241	5750	35	6550	70	Unspecified plant fragments and insect chiton
117538	Core 1 255	263–264	6205	35	7095	130	Unspecified plant fragments and insect chiton
117539	Core 1 265	273–274	7415	40	8255	60	Unspecified plant fragments and minor chiton
120880	Wood from North Goat Outlet Glacier valley	n.a.	415	35	480	85	Outer rings of subfossil tree trunk

[a] CAMS, analyses performed at the Center for Accelerator Mass Spectrometry, Lawrence Livermore National Laboratory.
[b] blf, below lake floor.
[c] Calibrated using CALIB 5.0 (Stuiver and Reimer, 1993).
[d] Identifications by R. S. Anderson (Northern Arizona University).
[e] Not used in age model; macrofossil was probably stored on the landscape for a prolonged interval prior to redeposition in the lake.

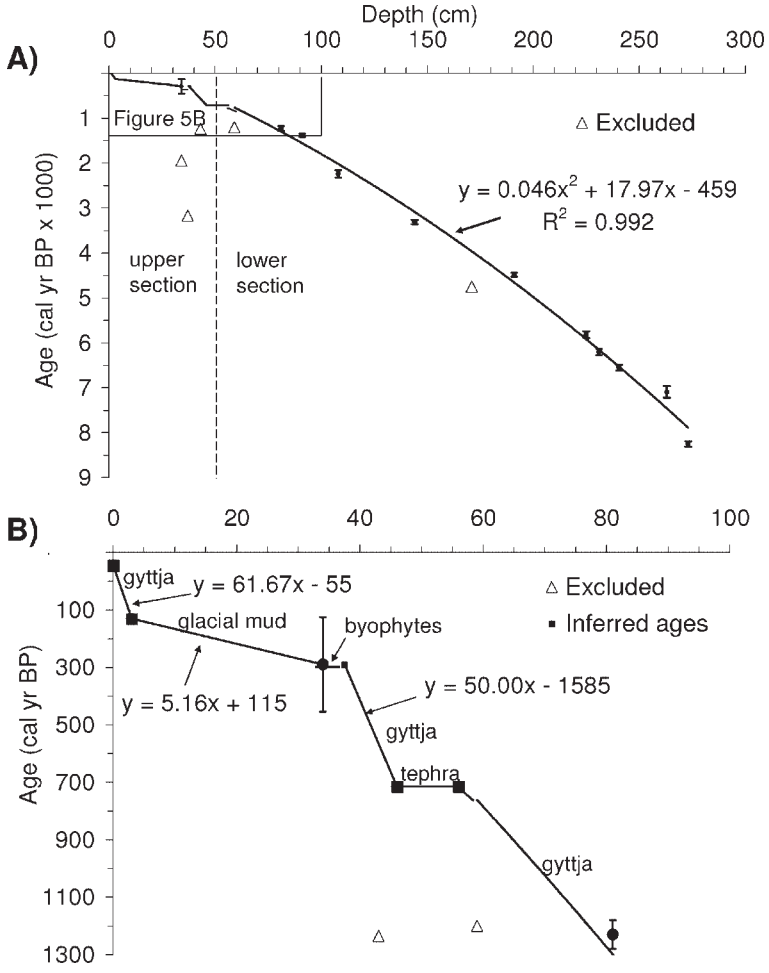

Figure 5 Age model for Goat Lake core 1. (A) The lower section of the core includes 10 ^{14}C ages fit with a second-order polynomial ($R^2 = 0.992$). Five ^{14}C ages were rejected because they are significantly older than expected based on neighbouring ages, probably because they contained old terrestrial material (see text). (B) The upper section (56–0 cm) was fitted to linear segments to account for shifts in sedimentation rates as described in the text

DOI: 10.1002/jqs

stratigraphic horizons identified at 9.5 cm depth in surface core 2C, and 1.5 cm in long core 1 (Daigle, 2006), indicate that the top of core 1 includes all the sediment except the upper 8 cm. All analyses above 8 cm were conducted on surface core 2C. The 3.74 m long composite record from core 1 was subdivided into four units (Fig. 6), including from bottom to top: (1) a 66 cm thick basal inorganic grey mud (7.5 YR 5/0) that fines upward with sporadic, weak, deformed laminations (374–308 cm depth); (2) a 10 cm thick transition zone (308–298 cm depth) that grades smoothly from grey, fine-grained inorganic mud (7.5 YR 5/0) into massive, brown organic-rich gyttja (10 YR 3/2), and exhibits a uniform increase in OM and BSi; (3) the primary sedimentary interval (298–40 cm depth), which overlies the transition zone, consists of massive, brown gyttja (10 YR 3/2), with abundant OM (typically 25%) and BSi (typically 30%), and marked by frequent interbeds of dark, detrital organic matter and at least 17 visible tephra layers; and (4) a 40 cm thick zone dominated by laminated, grey inorganic mud with thin beds of organic-rich mud (40–0 cm depth).

In detail, the stratigraphy of the upper 40 cm is marked by sharp stratigraphic transitions reflecting the influence of the NGG on Goat Lake. Two separate 1 mm thick inorganic grey layers around 40 cm are overlain by 3 cm of detrital terrestrial vegetation, which in turn is overlain by 31 cm of distinctly laminated (1–5 mm thick laminations), inorganic grey mud (5 Y 4/1) with interbeds of darker organic-rich material. The lamination composition ranges from clay- and silt-rich layers to organic-rich layers containing abundant plant macrofossils. The uppermost 3 cm is a massive, brown gyttja similar to the primary sedimentary unit. OM and BSi in the upper 40 cm fluctuate sharply between 5% and 20%, reflecting interbeds of inorganic grey sediment, gyttja, and bryophytes.

Core 2 penetrated deeper than core 1 and contains nearly identical stratigraphy, confirming the congruity of the stratigraphic record (Daigle, 2006). An additional 2 m of non-laminated coarse sand, silt, and clay with angular to sub-rounded clasts ranging from 0.5 to 5.0 cm in diameter were recovered in core 2. Some of the larger clasts are striated. Seventeen discrete tephra beds were located visually in the cores (Fig. 6). They range in thickness from 1 to 250 mm. The tephra at 165–166 cm depth contains laminations, biotite and a colour sequence that have been used to identify the Hayes

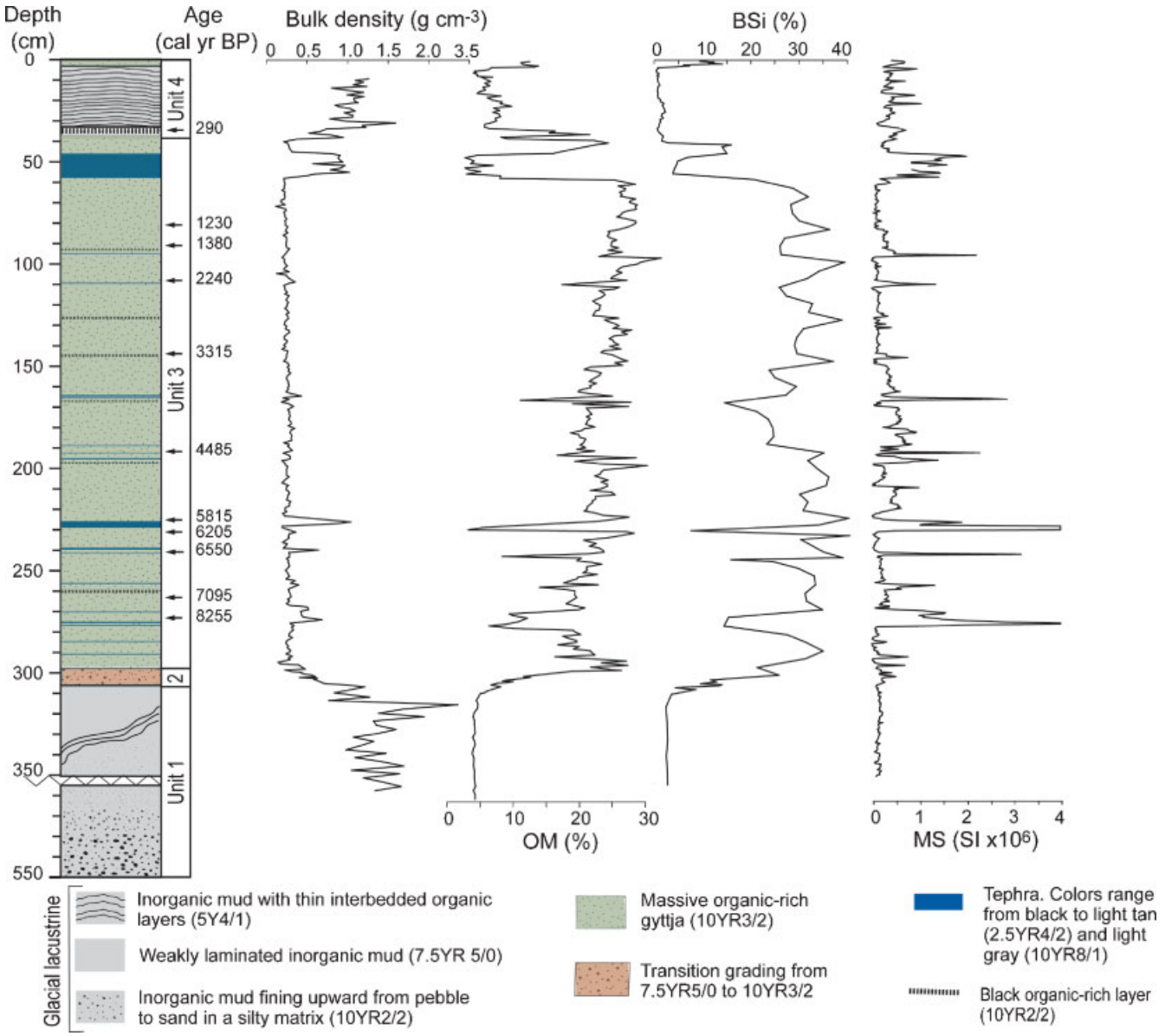

Figure 6 Core 1 lithology showing major units described in the text and all sediment proxies. OM, organic matter content based on loss on ignition; BSi, biogenic silica (SiO_2%); MS, magnetic susceptibility. Radiocarbon ages are calibrated to calendar years before 1950 (cal. yr BP; data listed in Table 2). This figure is available in colour online at www.interscience.wiley.com/journal/jqs

DOI: 10.1002/jqs

tephra around Cook Inlet (Riehle, 1994). Published ^{14}C ages show that the Hayes tephra was erupted between 3500 and 3800 cal. yr BP (Riehle *et al.*, 1990), which is consistent with the Goat Lake age model, which yields an age of 3700 cal. yr BP for the tephra.

Early to middle Holocene glacial and lacustrine history

Unit 1 in the lower 66 cm of core 1 is interpreted as ice-proximal, glacial-lacustrine sediment. Extrapolating the polynomial age model down to the top of the glacially influenced sediment at 308 cm yields an age of 9500 cal. yr BP. This is 1000 yr later than a near-basal age (10 550 cal. yr BP) on peat from an interior valley of the Kenai Mountains (9310 ± 200 ^{14}C yr. BP; Ager, 2001). The NGG apparently remained more extensive than present through the last glacial–interglacial transition, and through the early Holocene thermal maximum. The acoustic stratigraphy suggests that the entire post-glacial sequence was recovered in the cores; it is unlikely that unit 1 was deposited during a re-advance.

The sedimentary transition (unit 2) above the glacial-lacustrine unit reflects the retreat of the NGG below the elevation of the drainage divide during the early Holocene, and a shift in trophic level as Goat Lake evolved from a cold, turbid, proglacial lake into a thermally stratified lake with no glacial influence.

Down-core variations in BSi and OM reflect a number of environmental factors including temperature, the duration of the ice-free season, nutrient and light availability, and dilution by the other organic and mineral matter (Battarbee, 2000). OM and BSi values increase rapidly upward through unit 2, attaining near-maxima of 20% and 25%, respectively. In unit 3, above the transition zone, a broad trough in OM values around 8000–7600 BP is followed by an overall rise up to the base of the thickest tephra around AD 1235, where they attain their highest values, around 25% (Fig. 6). Trends in BSi largely parallel OM, suggesting increased productivity in the lake or drainage basin. Minor, short-lived peaks might reflect intermittent decades of warmer conditions whereas troughs generally coincide with tephras.

Glacier expansions in southern Alaska may have begun as early as 6000 cal. yr BP in the St Elias Mountains (Calkin *et al.*, 2001) and Neoglaciation was underway by 3600 cal. yr BP on the Kenai Peninsula (Wiles and Calkin, 1994). The cooler summer temperature that drove early Neoglacial ice advance (Calkin *et al.*, 2001; Wiles *et al.*, 1998, 2008) is not apparent in the OM and BSi data from Goat Lake (Fig. 6), suggesting that they reflect factors other than temperature. The extent of glaciers in the Kenai Mountains during the early–middle Holocene is not known, except the NGG did not expand to reach the drainage divide during this interval.

Little Ice Age glacial and lacustrine history

The series of sedimentary transitions above 40 cm in core 1 (unit 4) are considered in conjunction with glacial-geological evidence from the NGG to reconstruct the glacier activity and sedimentary response during the LIA. In the NGG valley, a ^{14}C age of 480 ± 85 cal. yr BP (about AD 1470) on the outer rings of a log 30 cm in diameter buried in till near the 2006 ice margin (Fig. 3) restricts the timing of glacier advance over this location. The log was abraded and the tree likely died following 480 cal. yr BP, but nonetheless adds to other evidence from Kenai Peninsula for glacier expansion during the mid 15th century (Wiles and Calkin, 1994; Wiles *et al.*, 2008).

In Goat Lake sediment, a 1 mm thick layer of rock flour signifies the first pulse of meltwater originating from the NGG upon its expansion to the elevation of the drainage divide. This layer likely corresponds to the deposition of the outer low-relief, grass-covered moraine near the drainage divide (Fig. 3). The initial rock flour is overlain by a 4 cm thick, bryophyte-rich layer that we interpret as a flood deposit generated by erosive meltwater that removed peat and carved a channel through the drainage divide. A ^{14}C age of 290 ± 165 cal. yr BP (about AD 1660) on wood fragments in the flood deposit from core 1 provides an approximate maximum age for the arrival of the NGG at the drainage divide. The bracketing ^{14}C ages from the buried log and lake sediment suggest that it took about 200 yr for the NGG to thicken 150 m from the elevation of the buried log, which is located perpendicular to the glacier flowline relative to the lowest point along the drainage divide at 590 m asl. The NGG never thickened much above the Goat Lake divide as indicated by the outermost glacier-marginal features that can be traced to the LIA terminal moraine 1.5 km down-valley.

The arrival of the NGG at the drainage divide at about 290 cal. yr BP (AD 1660) coincides with the well-documented middle phase of the LIA in southern Alaska from about AD 1600 to 1715 (Calkin *et al.*, 2001; Wiles *et al.*, 2008), and suggests that the climate was more favourable for glaciation than it had been since 9500 cal. yr BP when meltwater was first extinguished from Goat Lake. The overall increase in the extent of glaciers during the Holocene, culminating late during the LIA, is consistent with the long-term decrease in summer insolation driven by orbital cycles (Porter, 2007). Climate changes on timescales of centuries have been correlated with solar variability (e.g. Beer *et al.*, 2000). In Alaska, glacier fluctuations of the LIA coincide with solar variability (Wiles *et al.*, 2004). The advance of the NGG around 480 cal. yr BP (AD 1470) occurred during the Sporer solar minimum, and its arrival at the drainage divide around 290 cal. yr BP (AD 1660) occurred during the Maunder solar minimum.

The 32 cm of laminated, inorganic mud that overlie the dated bryophyte-rich flood deposit record the uninterrupted input of glacial meltwater during the maximum LIA. Fluctuations of the NGG during the 250 yr interval during which it occupied the drainage divide are not discernible in the sedimentary sequence. The position of the NGG is instead interpreted from glacial-geological features at the drainage divide and documentary evidence of the ice-marginal position. Lichen ages on the outwash bars and inset moraines indicate that these deposits stabilised around 50 cal. yr BP (AD 1900), about the same time as maximum LIA moraines elsewhere around the Kenai Mountains, especially on the east side (Wiles and Calkin, 1994). Between about 1900 and 1950 AD, the NGG retreated 500 m up-valley and lowered by ~40 m at the drainage divide. Between 1950 and 2006, it retreated another 1 km and lowered 150 m below the drainage divide. The average retreat rate during the 20th century was 15 m yr^{-1}, similar to other Harding Icefield outlet glaciers during the same time (Wiles and Calkin, 1994).

Although the dated log in the NGG valley was not in its original growth position, the tree must have lived near the site, or somewhere farther up-valley, requiring ice-free conditions in the decades before 480 cal. yr BP. Buried logs, exposed logs

DOI: 10.1002/jqs

and patches of organic soil were observed at three other locations near the modern ice margin (Fig. 3), indicating that a forest occupied the NGG valley at the present location of the ice margin during the 15th century. The forest was likely initiated during medieval times, suggesting warmer temperatures and restricted ice. On the other hand, the inferred warmer temperature during medieval times (Calkin *et al.*, 2001; Wiles and Calkin, 1994; Wiles *et al.*, 2008) is not apparent in the Goat Lake productivity signal. Nor does Goat Lake sediment document the well-known cooling and glacier advance during the first millennium AD, centred around AD 600 (Reyes *et al.*, 2006). It does, however, demonstrate that the NGG reached its Holocene maximum extent in the 17th century, late during the LIA.

Tree rings

A Swedish increment borer was used to remove a 5 mm diameter core at chest height from 29 living mountain hemlock trees within 0.5 km of Goat Lake in July 2005. Two trees were cored twice, two trees were discarded from the chronology because the crown had been damaged and two trees were discarded due to poor core retrieval. Cores were processed using standard procedures (Fritts, 1976). In all, 25 cores from 23 trees were included to build a chronology, which was constructed using COFECHA (Grissino-Mayer *et al.*, 1997). Visual checks were made to ensure correct cross dating. The Expressed Population Signal with an applied threshold value of 0.85 (Wigley, 1984) was used to determine that seven trees are required to maintain a statistically significant chronology at Goat Lake. The series was detrended using horizontal straight-line standardisation.

The Goat Lake tree-ring chronology provides a continuous record of ring width from AD 1723 to 2005 (Fig. 7). It correlates with May through August temperature at Kenai ($r = 0.35$; $P = 0.008$; Daigle, 2006). The ring-width series from Goat Lake is also strongly correlated ($r = 0.54$, $P = 6.81 \times 10^{-21}$) with the series from Exit Glacier located 20 km south-east of Goat Lake (Wiles *et al.*, 1998), indicating that trees at Goat Lake respond to regional climate. Additionally, ring-width series from different sites around the Gulf of Alaska are strongly correlated, suggesting that they also respond coherently to climate conditions across the gulf (Wiles *et al.*, 1995, 1998). Further evidence that the trees in the Goat Lake watershed respond to regional climate is the observed shift to cooler conditions in the 1940s and to warmer conditions in 1976 associated with shifts in the AL index (Francis and Hare, 1994; Wiles *et al.*, 1998). The only unexpected feature of the Goat Lake ring-width series is the pronounced peak in ring width from about AD 1920 to 1940, which exceeds the magnitude measured at other sites (Wilson *et al.*, 2007). Instrumental records at Seward airport (Western Regional Climate Center, 2006) do not show highly elevated summer temperatures during this interval. The large ring widths in the Goat Lake series might indicate a growth release related to some forest disturbance, or to the lowering of the NGG surface to an elevation at which it could no longer drain cold air into the Goat Lake valley.

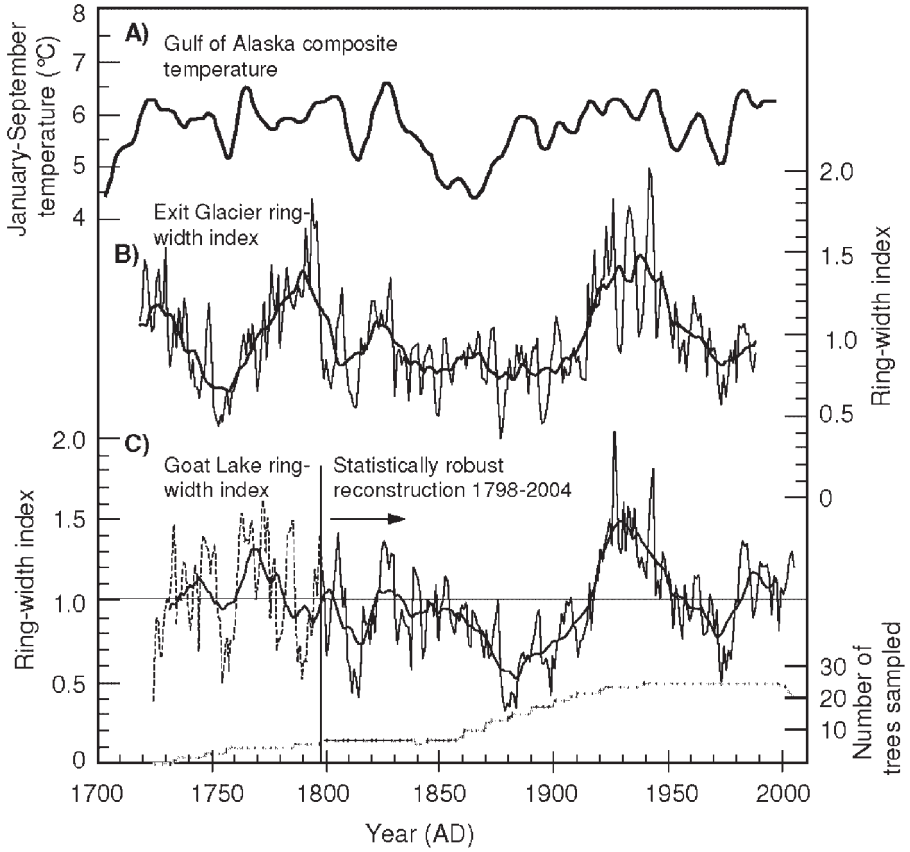

Figure 7 Goat Lake tree-ring series compared with other local and regional series. (A) January to September temperature reconstruction of surface air temperature based on tree-ring widths from locations around the Gulf of Alaska, showing 15 yr smoothed spline (Wilson *et al.*, 2007). (B) Tree-ring series from Sitka spruce trees near Exit Glacier detrended using horizontal straight-line standardisation similar to the Goat Lake series. Bold line is a 15 yr running mean. Data from the International Tree Ring Data Bank (2006). (C) Tree-ring series from mountain hemlock trees around Goat Lake. Bold line is a 15 yr running mean. Dashed line represents the series based on fewer than seven trees

DOI: 10.1002/jqs

Nonetheless, the Goat Lake tree-ring series is similar to those from other sites around the Gulf of Alaska (Fig. 7). Rather than relying on our single ring-width series from Goat Lake to reconstruct temperature changes, we use the more extensive suite of integrated regional analyses. Ring widths in trees around the Gulf of Alaska are primarily controlled by spring and summer temperatures (Wiles *et al.*, 1995, 1998; Barclay *et al.*, 1999; D'Arrigo *et al.*, 1999; Davi *et al.*, 2003). Tree-ring-based spring and summer temperature reconstructions (March–September) around the Gulf of Alaska indicate a sustained temperature lowering of approximately 1.0°C during the second half of the 19th century compared to the first half of the 20th century (Wiles *et al.*, 1998; D'Arrigo *et al.*, 1999; Wilson *et al.*, 2007). We adopt this estimate as the LIA ablation-season temperature lowering at our site. The reference period for this temperature change (the first half of the 20th century) generally coincides with the reference period for the ΔELA value, which is based on glacier geometry in the 1950s.

Winter precipitation and controls on glacier expansion

Because glacier size depends primarily on the counterbalancing effects of ablation-season temperature and winter accumulation (Sutherland, 1984), we can use the estimated ablation-season temperature lowering along with our ΔELA value to infer changes in winter precipitation during the LIA maximum. Assuming that the shift in temperature is directly related to a shift in the ELA, and that winter precipitation remained constant (which is unlikely), then a 1°C temperature change should correspond to a ΔELA of 170 m. This value is based on an adiabatic lapse rate of 6.0°C km^{-1}, which was determined using daily air-temperature data from Kenai (3 m asl), Goat Lake[1] (550 m asl), Wolverine Glacier (900 m asl) and the Harding Icefield (1200 m asl) from April to August 2006 (Daigle, 2006). In contrast, our analysis shows that ΔELA was probably restricted to 34 m, and no more than 60 m. Therefore, a reduction in winter precipitation seems to be required to reconcile the difference. Quantifying the amount of precipitation reduction will require a modelling study to assess the relative importance of summer temperature and winter precipitation on the mass balance of Kenai Mountain glaciers.

The restricted ELA lowering in cirques around Goat Lake during the maximum LIA suggests that cooler temperatures were accompanied by decreased winter accumulation, implying a generally weakened AL. Our limited lichenometric ages, together with the more extensive work in the Kenai Mountains by Wiles and Calkin (1994), indicate that most glaciers reached their maximum LIA extents late in the 19th century, around the time of the lowest summer temperatures in the tree-ring series, suggesting that summer cooling overshadowed the effect of decreased winter accumulation on glacier mass balance. A reconstruction of the relative intensity of the AL over the past 4000 yr from lacustrine carbonate in the Yukon Territory (Anderson *et al.*, 2005) shows that the weakest AL occurred from 100 to 800 and 1800 AD. Snowfall on Mt Logan in southwestern Yukon Territory correlates with the strength of the AL and also shows generally lower precipitation during the 19th century (Rupper *et al.*, 2004): further evidence for a weakened AL during the maximum LIA.

[1]The Goat Lake temperature is based on a temperature logger and radiation shield that we installed in a tree at the northern end of the lake in June 2004 (data available at http://jan.ucc.nau.edu/~dsk5/S_AK/).

Although summer temperature seems to be the dominant control on glacier expansion around Goat Lake, mass-balance data from Wolverine Glacier shows a positive response to increased winter precipitation from 1976 to 1990 (Mayo and March, 1990). The increased winter precipitation and positive mass balance corresponds to the shift from a generally weak to a generally strong AL after 1976 (Francis and Hare, 1994). Other glacier records in comparison with tree-ring temperature reconstructions reveal the variable influence of temperature and winter precipitation on glacier activity around the Gulf of Alaska (D'Arrigo *et al.*, 2005; Wiles *et al.*, 2008). Wiles *et al.* (2008) identified three phases of LIA glacier advance that all correlate with decreased summer temperatures based on tree-ring studies by Barclay *et al.* (2003) and Davi *et al.* (2003). D'Arrigo *et al.* (2005) evaluated tree-ring series from around the Gulf of Alaska and correlated the middle LIA expansion with relatively strong (wet) AL, and the late LIA expansion with a relatively weak (dry) AL.

Summary and conclusions

Lake sediment, tree rings and glacier fluctuations in the Goat Lake area of the Kenai Mountains were studied to infer Holocene climate changes. Our limited ^{14}C and lichenometric ages agree with the extensive previous work on late Holocene glacier fluctuations in the area (Wiles and Calkin, 1994; Wiles *et al.*, 2008), and fill a gap in coverage of the glacial geology along the northern Harding Icefield. A glacially overrun log at the 2006 ice margin of NGG yielded an age of about 480 cal. yr BP (AD 1470), indicating that the NGG had advanced to its current location by that time. An abrupt shift from organic-rich gyttja to clay- and silt-rich rock flour occurred around 290 cal. yr BP (AD 1660) in Goat Lake sediment, and signifies the first time since 9500 cal. yr BP that the NGG occupied drainage divide that otherwise separates the glacier from Goat Lake. Lichen ages on moraines and outwash bars at the drainage divide indicate that the ice remained at the divide until around 50 cal. yr BP (AD 1900). Since that time, the NGG has thinned 150 m, retreated 1.5 km, and Goat Lake has returned to a non-glacial lake accumulating 3 cm of gyttja above the LIA rock flour.

ELAs reconstructed using the AAR method and photo-interpretative mapping at 12 cirques near Goat Lake indicate a lowering of 34 m, and no more than 60 m during the maximum LIA compared with the glaciological conditions represented by the AD 1950 glacier margins. A 34–60 m ΔELA is consistent with other estimates from south-west Alaska, but is two to five times less than estimates from ice fields and valley glaciers on the Kenai Peninsula. The topographically confined glaciers used in this study should provide an accurate approximation of ΔELA.

A regionally consistent tree-ring series from mountain hemlock trees around Goat Lake support an average spring/summer temperature lowering of about 1°C during the coldest decades of the 19th century compared to the early 20th century (the interval that is likely reflected in the 1950 configuration of the cirque glaciers). Assuming that winter accumulation did not change, a 1°C temperature reduction should correspond to a ΔELA of 170 m during the LIA. Because the inferred ΔELA is much less, a decrease in winter precipitation is needed to reconcile the restricted ELA lowering during the 19th century. Instrumental data show that decreased winter precipitation around the Gulf of Alaska is related to a weakening of the AL. Because glaciers attained their maximum LIA extents during

DOI: 10.1002/jqs

intervals of decreased winter precipitation, this glacier expansion is attributed to decreased ablation. Therefore summer temperature seems to be the dominant factor influencing centennial-scale glacier fluctuations in this part of the Kenai Mountains and possibly elsewhere in southern Alaska, as has been suggested previously (e.g. Wiles *et al.*, 2008).

Our lake-core evidence places the LIA in the context of a longer time series that highlights the maximum extent of Holocene glaciers during the 17th to 19th centuries. This first-order trend probably reflects broad-scale forcing by orbital cycles that drive summer insolation. The extent to which this forcing also controlled long-term cyclonic activity in the northeastern Pacific is not well known.

Acknowledgements We thank Al Werner and R. Scott Anderson for their helpful suggestions during all phases of this research. They helped core Goat Lake, along with K. Kathan and E. Dopfel, and they provided input to Daigle's master's thesis, along with M. Ort. E. Berg identified the bryophytes and facilitated our research on the Kenai National Wildlife Refuge. M. Hamilton, C. Kassel, N. McKay and C. Schiff assisted in the field. K. Wallace at the USGS/Alaska Volcano Observatory analysed the tephra, and T. Brown at the Lawrence Livermore National Laboratory analysed radiocarbon ages with funding from the USGS/Alaska Volcano Observatory. The tree rings were analysed with the generous support of Northern Arizona University's Ecological Restoration Institute, and the data were analysed with the guidance of G. Wiles. We thank G. Wiles and C. Waythomas for their insightful and constructive reviews. This research was funded by the National Science Foundation (ATM-0318341) and the Geological Society of America.

References

Ager TA. 2001. Holocene vegetation history of the northern Kenai Mountains, south-central Alaska. *US Geological Survey Professional Papers* **1633**: 91–108.

Anderson L, Abbott MA, Finney BP, Burns SJ. 2005. Regional atmospheric circulation change in the North Pacific during the Holocene inferred from lacustrine carbonate oxygen isotopes, Yukon Territory, Canada. *Quaternary Research* **64**: 21–35.

Barclay DJ, Wiles GC, Calkin PE. 1999. A 1119-year tree-ring-width chronology from western Prince William Sound, southern Alaska. *The Holocene* **9**: 79–84.

Barclay DJ, Wiles GC, Calkin PE. 2003. An 850 year record of climate and fluctuations of the iceberg-calving Nellie Juan Glacier, south central Alaska, USA. *Annals of Glaciology* **36**: 51–56.

Battarbee RW. 2000. Palaeolimnological approaches to climate change, with special regard to the biological record. *Quaternary Science Reviews* **19**: 107–124.

Beer J, Mende W, Stellmacher R. 2000. The role of the sun in climate forcing. *Quaternary Science Reviews* **19**: 403–415.

Benn DI, Owens LA, Osmaston HA, Seltzer GO, Porter SC, Mark B. 2005. Reconstruction of equilibrium-line altitudes for tropical and sub-tropical glaciers. *Quaternary International* **138–139**: 8–21.

Calkin PE, Ellis JM. 1980. A lichenometric dating curve and its application to Holocene glacier studies in the central Brooks Range, Alaska. *Arctic and Alpine Research* **12**: 245–264.

Calkin PE, Wiles GC, Barclay DJ. 2001. Holocene coastal glaciation of Alaska. *Quaternary Science Reviews* **20**: 449–461.

Daigle T. 2006. *Late Holocene climate change at Goat Lake, Kenai Mountains, south-central Alaska*. MS thesis, Northern Arizona University, Flagstaff, AZ.

D'Arrigo R, Wiles G, Jacoby G, Villalba R. 1999. North Pacific sea surface temperatures: past variations inferred from tree rings. *Geophysical Research Letters* **26**: 2757–2760.

D'Arrigo R, Wilson R, Deser C, Wiles G, Cook E, Villalba R, Tudhope AW, Cole J, Linsley B. 2005. Tropical-North Pacific climate linkages over the past four centuries. *Journal of Climate* **18**: 5253–5265.

Davi NK, Jacoby GC, Wiles GC. 2003. Boreal temperature variability inferred from maximum latewood density and tree-ring width data, Wrangell Mountain region, Alaska. *Quaternary Research* **60**: 252–262.

Dyurgerov M. 2002. Glacier mass balance and regime: data of measurements and analysis. *INSTAAR Occasional Paper no.* 55, University of Colorado.

Francis RC, Hare SR. 1994. Decadal scale regime shifts in the large marine ecosystems of the North East Pacific: a case for historical science. *Fisheries and Oceanography* **3**: 279–291.

Fritts HC. 1976. *Tree Rings and Climate*. Academic Press: New York.

Grissino-Mayer HD, Holmes RL, Fritts HC. 1997. *The International Tree-Ring Data Bank Program Library*, Version 2.1. Users Manual. Tucson, AZ.

Hu FS, Kaufman D, Yoneji S, Nelson D, Shemesh A, Huang Y, Tian J, Bond G, Clegg B, Brown T. 2003. Cyclic variation and solar forcing of Holocene climate in the Alaskan subarctic. *Science* **301**: 1890–1892.

International Tree Ring Databank. 2006. Tree-ring search engine. http://www.ncdc.noaa.gov/paleo/treering.html [August 2005].

Kathan KM. 2006. Late Holocene climate fluctuations at Cascade Lake, Ahklun Mountains, southwestern Alaska. MS thesis, Northern Arizona University, Flagstaff, AZ.

Levy LB, Kaufman DS, Werner A. 2004. Holocene glacier fluctuations, Waskey Lake, northeastern Ahklun Mountains, southwestern Alaska. *The Holocene* **14**: 185–193.

Mayo LR, March RS. 1990. Air temperature and precipitation at Wolverine Glacier, Alaska: glacier growth in a warmer, wetter climate. *Annals of Glaciology* **14**: 191–194.

McKay N. 2007. Late Holocene climate at Hallet and Greyling Lakes, central Chugach Range, south-central Alaska. MS thesis, Northern Arizona University, Flagstaff, AZ.

Minobe S, Mantua N. 1999. Interdecadal modulation of interannual atmospheric and oceanic variability over the North Pacific. *Progress in Oceanography* **43**: 163–192.

Mortlock RA, Froelich PN. 1989. A simple method for the rapid determination of biogenic opal in pelagic marine sediments. *Deep-Sea Research. Part A: Oceanographic Research Papers* **36**: 1415–1426.

Nesje A, Dahl SO, Lie O. 2004. Holocene millennial-scale summer temperature variability inferred from sediment parameters in a non-glacial mountain lake: Danntjørn, Jotunheimen, central southern Norway. *Quaternary Science Reviews* **23**: 2183–2205.

Osborn G, Menounos B, Koch J, Clague JJ, Vallis V. 2007. Multi-proxy record of Holocene glacial history of the Spearhead and Fitzsimmons ranges, southern Coast Mountains, British Columbia. *Quaternary Science Reviews* **26**: 479–493.

Overland JE, Adams JM, Bond NA. 1999. Decadal variability of the Aleutian low and its relation to high-latitude circulation. *Journal of Climate* **12**: 1542–1548.

Padginton CH. 1993. A Little Ice Age reconstruction for ice tongues of the Grewingk-Yalik Ice Complex, southern Kenai Mountains, Alaska. MS thesis, University of New York at Buffalo, NY.

Papineau JM. 2001. Wintertime temperature anomalies in Alaska correlated with ENSO and PDO. *International Journal of Climatology* **21**: 1577–1592.

Porter SC. 2007. Neoglaciation in the American Cordilleras. In *Encyclopedia of Quaternary Science*, Elias SA (ed.). Elsevier: Oxford; 1133–1142.

Reyes AV, Wiles GC, Smith DJ, Barclay DJ, Allen S, Jackson S, Larocque S, Laxton S, Lewis D, Calkin PE, Clague JJ. 2006. Expansion of alpine glaciers in Pacific North America in the first millennium AD. *Geology* **34**: 57–60.

Riehle JR. 1994. Heterogeneity, correlative, and proposed stratigraphic nomenclature of Hayes tephra set H, Alaska. *Quaternary Research* **41**: 285–288.

Riehle JR, Bowers PM, Ager TA. 1990. The Hayes tephra deposits, an upper Holocene marker horizon in south-central Alaska. *Quaternary Research* **33**: 276–290.

Rodionov SN, Overland JE, Bond NA. 2005. The Aleutian low and winter climatic conditions in the Bering Sea. Part 1: classification. *Journal of Climate* **18**: 160–177.

Rupper S, Steig E, Roe G. 2004. The relationship between snow accumulation at Mt Logan, Yukon, Canada, and climate variability in the North Pacific. *Journal of Climate* **17**: 4724–4739.

Solomina O, Calkin PE. 2003. Lichenometry as applied to moraines in Alaska, USA, and Kamchatka, Russia. *Arctic Antarctic and Alpine Research* **35**: 129–143.

Stuiver M, Reimer PJ. 1993. Extended ^{14}C database and revised CALIB radiocarbon calibration program. *Radiocarbon* **35**: 215–230.

Sutherland DG. 1984. Modern glacier characteristics as a basis for inferring former climates with particular reference to the Loch Lomond stadial. *Quaternary Science Reviews* **3**: 291–309.

Western Regional Climate Center. 2006. Seward and Kenai meteorological stations. Alaska climate summaries section. http://www.wrcc.dri.edu/summary/climsmak.html [13 September 2006].

Wigley TML, Briffa KR, Jones PD. 1984. On the average value of correlated time series, with applications in dendroclimatology, and hydrometeorology. *Journal of Applied Climatology and Meteorology* **23**: 201–213.

Wiles GC. 1992. Holocene glacier fluctuations in the southern Kenai Mountains. PhD thesis, University of New York at Buffalo, NY.

Wiles GC, Calkin PE. 1993. Neoglacial fluctuations and sedimentation of an iceberg-calving glacier resolved with tree rings (Kenai Fjords National Park, Alaska). *Quaternary International* **18**: 35–42.

Wiles GC, Calkin PE. 1994. Late Holocene, high-resolution glacial chronologies and climate, Kenai Mountains, Alaska. *Geological Society of America Bulletin* **106**: 281–303.

Wiles GC, D'Arrigo RD, Jacoby GC. 1995. Modeling North Pacific temperature and pressure changes from coastal tree-ring chronologies. In *Proceedings from the 11th Annual Pacific Climate Workshop*, Isaacs CM, Tharp VL (eds); 67–78.

Wiles GC, D'Arrigo RD, Jacoby GC. 1998. Gulf of Alaska atmosphere-ocean variability over recent centuries inferred from coastal tree-ring records. *Climate Change* **38**: 289–306.

Wiles GC, D'Arrigo RD, Villalba R, Calkin PE, Barclay DJ. 2004. Century-scale solar variability and Alaskan temperature change over the past millennium. *Geophysical Research Letters* **31**: L15203.

Wiles GC, Barclay DJ, Calkin PE, Lowell TV. 2008. Century to millennial-scale temperature variation for the last two thousand years inferred from glacial geologic records of southern Alaska. *Global and Planetary Change* **60**: 115–125.

Wilson R, Wiles G, D'Arrigo R, Zweck C. 2007. Cycles and shifts: 1,300 years of multi-decadal temperature variability in the Gulf of Alaska. *Climate Dynamics* **28**: 425–440.